Research on Engineering Structures & Materials
www.jresm.org
Research Group

Research Article

Study and analysis of vibration and mechanical characteristics of PVC-carbon fiber-graphene nanocomposite pipes designed for oil and gas applications

Salah Khudhur Mohammad [*,a]

Ministry of Oil, Midland Refineries Company, Baghdad, Iraq

Article Info

Article History:

Received 14 Oct 2025

Accepted 05 Dec 2025

Keywords:

Graphene;
Mechanical properties;
The natural frequencies;
Gas oil;
Nanocomposite pipe

Abstract

This paper presents an innovative plastic injection molding technique for producing polyvinyl chloride/carbon fiber/graphene nanocomposite pipes. It includes calculating the natural frequencies and vibration properties of the composite pipe under various flow velocities of (Gas oil) fluid with a density of 0.822 g/cm^3. The mechanical performance of the fabricated composite nano pipes is evaluated using three tests: axial tensile, axial compression stress, and ultimate strain. Young's modulus varies, ranging between 40 GPa and 120 GPa depending on the composite metal's percentage of polyvinyl chloride/ carbon fiber/ graphene. Mathematical results using MATLAB demonstrate that the reprocessed PVC/CF/Gr composites demonstrated superior mechanical performance relative to (FEM) predictions in the Ansys software workbench 21.0 package. Specifically, a 170% increase in Young's modulus and a 140% increase in ultimate tensile strength were observed at 2 wt% graphene. Due to the bonding between the fibers and the polymer matrix, the highest difference in the fundamental natural frequency between the theoretical and numerical results was found to be 8.18%, at a speed of 2 m/s.

1. Introduction

1.1. Describing the New Technique and Objective

This article examines the study and analysis of fiber-reinforced nanocomposite pipes. A series of tests was conducted to evaluate their mechanical and vibrational properties, including axial tension, transverse compression, and axial compression, in order to assess their effects on the ultimate tensile strength and Young's modulus of the nanocomposite pipes. Since high tensile strength is a crucial requirement for oil and gas pipelines, the study focuses on enhancing the mechanical durability of these pipes so they can withstand the stress levels typically endured by steel pipes used in such applications. This is achieved by analyzing the fundamental natural frequencies of the pipes and their vibrational behavior during fluid flow at various flow velocities.

Nanomaterials have emerged as a transformative advancement in modern materials science, owing to their exceptional mechanical, thermal, and chemical properties. Among these, polymer-based nanocomposites have attracted significant attention due to their versatile performance, ease of fabrication, and cost-effectiveness. Nanocomposite pipes exhibit high mechanical strength, excellent thermal stability, and notable defect tolerance, rendering them highly suitable for oil and gas transportation systems, while also offering economic advantages. Furthermore, nanocomposite coatings have been demonstrated to provide effective corrosion protection in harsh operational environments within the oil and gas industry [1].

*Corresponding author: 200saaa200@gmail.com
[a]orcid.org/0009-0001-6887-7322
DOI: http://dx.doi.org/10.17515/resm2025-1263ic1014rs

Reinforcement materials such as titanium dioxide, zinc oxide, carbon nanotubes (CNTs), and graphene (Gr) are widely employed due to their superior mechanical and thermal characteristics. Pohasem et al. reported significant improvements in corrosion resistance through the incorporation of steel–epoxy–graphene composites [2,3]. Pipelines are inherently subjected to internal and external stresses induced by fluid flow, which may lead to structural degradation or failure. Consequently, dynamic analysis is critical to ensure operational reliability and structural integrity. Modeling approaches typically rely on vibration velocity data to quantify reductions in structural stiffness, with S.M. Shankaraachhar and colleagues developing a comprehensive mathematical framework to investigate the vibration behavior and stability of fluid-conveying pipelines [4,5]. Recent studies have further demonstrated the effectiveness of nanocomposites in corrosion and thermal protection.

TabkhPaz et al. showed that double-layer coatings of steel, reinforced with graphene, CNTs, and zinc particles, significantly enhance corrosion resistance [6]. Similarly, Yu et al. reported that polystyrene/graphene nanocomposites provide excellent resistance against both corrosion and heat [7]. Liu et al. investigated single-layer graphene coatings on epoxy primers, identifying 2 wt% graphene as an optimal ratio for cathodic protection, which improved the corrosion resistance of polystyrene from 37.9% to 99.53% and increased thermal resistance by 24.8% [8,9]. Samsudin et al. examined the thermal and mechanical properties of thermoset polyethylene/graphite nanocomposites, noting that a graphite content of 0.1 wt% increases crystallinity by 15% [10]. The thermal properties of epoxy composites reinforced with carbon fibers were further enhanced by adding 0.3 wt% graphene oxide, which doubled the storage modulus of the composites [11]. Karsli et al. demonstrated that surface treatment of CNTs improves the mechanical and electrical properties of polypropylene/short glass fiber composites [12,13], while Prusty et al. confirmed that the inclusion of glass fibers and CNTs enhances elasticity and the modulus of elasticity [14].

Despite these advancements, aggregation of nanomaterials remains a key challenge in nanocomposite fabrication. Patel et al. investigated the effect of increasing CNT content in epoxy/fiberglass composites, finding that concentrations up to 1 wt% improve tensile and flexural strength, whereas higher contents lead to aggregation that adversely affects mechanical properties [15,16]. The method of Nano filler incorporation further affects composite properties. Brandenburg et al. compared melt mixing and solution mixing in polyethylene composites and found that CNTs are more uniformly dispersed in nanocomposites prepared via melt mixing [17]. Aldajah and Haik employed a magnetic field to align CNTs in carbon fiber-reinforced composites, resulting in increases in flexural stiffness by 33% and 15%, respectively [18]. Saad et al. developed polyvinyl chloride (PVC)-based composites using various yarns and nanofillers to enhance PVC properties [19]. Nawaz et al. reported that incorporating 1.5 wt% nanofiller via an ordered mixing technique increased the modulus of elasticity by 62% and improved plastic quality by 20% [20,21]. Xiao et al. investigated PVC/graphene composites with graphene concentrations ranging from 1% to 9%, finding homogeneous dispersion at 1–5 wt% and explored higher graphene content in a polyvinyl chloride matrix and reported a 115% improvement in tensile strength at 5 wt% graphene concentrations. However, using high concentrations of graphene is not economically viable. Furthermore, graphene's tendency to agglomerate at higher wt% concentrations degrade the quality of the resulting nanocomposite, making it unsuitable for industrial applications [22].

Blending and recycling strategies also play a role in enhancing composite performance. Kuram et al. studied PBT/PC blends reinforced with recycled glass fibers and observed improved mechanical properties compared to virgin PBT/PC blends [23]. Kadam and Mhaske reported that three-cycle material recovery in nylon 6/talc nanocomposites increased tensile strength by 36.7% and tensile modulus by 169.7% during the extrusion cycle [24]. Collectively, these studies highlight the significant potential of nanomaterials to enhance the mechanical, thermal, and corrosion resistance properties of polymer-based composites, coatings, and pipeline systems. The performance of these materials is strongly influenced by several key factors, including the type and concentration of nanofillers, dispersion techniques, surface modification, and recycling strategies. Nevertheless, challenges such as nanomaterial agglomeration, long-term stability under operational loading, and the optimization of composite formulations remain critical areas requiring further investigation.

Given that high tensile strength is a fundamental requirement for oil and gas pipelines, this study focuses on enhancing the mechanical integrity of composite pipes to achieve strength levels comparable to those of conventional steel pipelines. Although this investigation was confined to small-diameter pipes, the findings provide promising evidence supporting the potential industrial adoption of composite pipes and their gradual replacement of traditional materials in oil and gas pipeline systems.

In this study, the addition of only 2 wt% graphene led to significant improvements in Young's modulus and tensile strength, by 170% and 140%, respectively. These results demonstrate the considerable potential for achieving substantial mechanical enhancements with relatively low graphene concentrations, highlighting their promise for industrial applications of composite nanotubes. This approach effectively leverages graphene's capacity to enhance the mechanical performance of nanocomposites. The findings further indicate that increasing the graphene content to 2 wt% improves the pipe's stiffness, with the most pronounced gains occurring at lower weight percentages, followed by a decline at higher percentages. Additionally, the maximum transverse load capacity of the nanocomposite pipes was evaluated for specimens showing pipe diameter displacements exceeding 5%, revealing that the pipe's ability to withstand transverse loads peaked at 2 wt% graphene. However, due to the weak adhesion between the fibers and the polymer matrix, fracture surfaces often revealed gaps around the fibers. These gaps led to stress concentration within the nanocomposite. By reinforcing the polymer matrix with graphene, this adhesion was significantly improved, filling the gaps and reducing stress concentration. Consequently, load transfer from the matrix to the fibers became more efficient. In contrast, the fibers detached from the matrix due to the weak load transfer, as they were torn and separated at the fracture surfaces.

2. The Analytical and Numerical Approach

2.1 Mathematical Modeling of Pipe

The equations of motion for the system are derived using the Euler–Bernoulli beam theory and subsequently solved to determine the fundamental natural frequency. This approach enables the analysis of free vibrations of a fluid-conveying reinforced pipe, under the assumptions of incompressible fluid flow and negligible effects of damping and gravity. The method is considered comprehensive, as it explicitly incorporates the pipe's stiffness characteristics into the dynamic model, providing a more accurate representation of its vibrational behavior.

2.2 Free Vibration

The Euler–Bernoulli equation governing a pipe conveying an incompressible fluid and subjected to an external force F_0, for pipes composed of PVC/CF/Gr, provides an accurate simulation of the free vibration behavior of fluid-conveying pipes with uniform cross-sections. The governing equation for such a pipe system is expressed as follows [25]:

$$\frac{d^2}{dx^2}\,EI\,\frac{d^2w}{dx^2} + 2mfV\frac{d^2w}{dxdt} + mf\frac{dv}{dt}\frac{dw}{dx} + (pA + mfV^2)\frac{d^2w}{dx^2} + (mf + mp)\frac{d^2w}{dt^2} = F_o \tag{1}$$

For the uniform cross-section area, the equation of pipe becomes,

$$EI\frac{d^4w}{dx^4} + 2mfV\frac{d^2w}{dxdt} + mf\frac{dv}{dt}\frac{dw}{dx} + (pA + mfV^2)\frac{d^2w}{dx^2} + (mf + mp)\frac{d^2w}{dt^2} = F_o \tag{2}$$

2.3 General Solution

Equation (2) describes the natural frequency of the composite nanotube as a function of the spatial coordinate x, capturing the variation of vibrational characteristics along the length of the pipe.

$$Y(T,X) = \sum_{j=1}^{4} Cje^{i\Omega T}e^{ij\lambda X} \tag{3}$$

Where: $\Omega = L\omega\sqrt{\frac{(mf+mp)}{EI}}$, $Y = \frac{pL^2A}{EI}$ $B = \sqrt[2]{\frac{mf}{mf+mp}}$, $U = VL\sqrt[2]{\frac{mf}{EI}}$

Subs. Eq. (3) into Eq. (2):

$$\lambda^4 - (Y + U^2)\lambda^2 - 2UB\Omega\lambda - \Omega^2 = 0 \quad (4)$$

Eq. (4) has four roots are:

$$\lambda_{1,2} = (-a \pm ib)1 = -\frac{1}{2}\sqrt{\alpha} \pm \frac{i}{2}\sqrt{\frac{4UB\Omega}{\sqrt{\alpha}} + \alpha - 2K} \quad (5)$$

$$\lambda_{3,4} = (a \pm b2) = \frac{1}{2}\sqrt{\alpha} \pm \frac{1}{2} \quad (6)$$

Where; $K = Y + U^2$, $\alpha = \frac{0.42S_1}{S_2} + 0.265S_2 + \frac{2}{3}K$, $S_1 = K^2 - 12\Omega^2$, $S_2 = (S + \sqrt{S^2 - 4S_1^3})^{0.333}$, $a = \frac{1}{2}\sqrt{\alpha}$, $b_1 = \frac{1}{2}\sqrt{\frac{4UB\Omega}{\sqrt{\alpha}} - 2K + \alpha}$, $b_2 = \frac{1}{2}\sqrt{\frac{4UB\Omega}{\sqrt{\alpha}} + 2K - \alpha}$

By analyzing the roots of Equation (4) and applying both algebraic and geometric simplifications, the resulting expression can be reduced to the following form:

$$W(T,X) = \left[H_1 e^{i(-a+ib_1)X} + H_2 e^{i(-a-ib_1)X} + H_3 e^{i(a+ib_2)X} + H_4 e^{i(a-ib_2)X}\right] e^{i\Omega T} \quad (7)$$

$$W(T,X) = \left[(H_1 e^{-b_1X} + H_2 e^{b_1X})e^{-iaX} + (H_3 e^{b_2X} + H_4 e^{-b_2X})e^{iaX}\right] e^{i\Omega T} \quad (8)$$

$$\sinh b_1X = e^{-b_1X}, \quad \cosh b_1X = e^{b_1X}, \quad \sin b_2X = e^{b_2X}, \quad \cos b_2X = e^{-b_2X}$$

Where; $A=H_1$ $B=H_2$ $D=H_3$ $E=H_3$

The solution for the vibration equation of a fluid-conveying pipe under conservative conditions is given by:

$$W(T,X) = \left[(A \sinh b_1X + B \cosh b_1X)e^{-iaX} + (D \sin b_2X + E \cos b_2X)e^{iaX}\right] e^{i\Omega T} \quad (9)$$

2.4 Solve the pipe Equation Motion

This section presents the derivation of Equation (9) to determine the natural frequency and the corresponding system response. The analysis incorporates the application of boundary conditions for a simply supported pipe, as illustrated in Figure 1. The initial conditions for the system can be expressed as follows:

$$w(x,0) = 0 \text{ (The pipe deflection)} \quad (10)$$

$$\frac{dw(x,0)}{dt} = 0 \text{ (The pipe moment)} \quad (11)$$

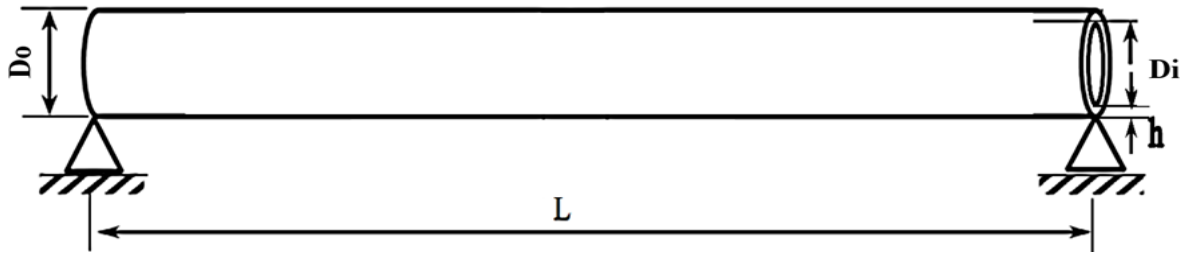

Fig. 1. The nanocomposite pipe

Simply supported B.C.S. at

- x =0 and x =L, w (0, t) = 0
- w (L, t) =0 ,

- $EI\ \frac{d^2\,w(t,x)}{dx^2} - M_P = 0$
- $EI\ \frac{d^3\,w(t,x)}{dx^3} - V_P = 0$

Where M_P (prescribed moment) and V_P (shear forces). The amplitude response of the pipe as a function of x can be obtained as follows:

$$W(X) = A\left(\left(sinh\, b_1X - \frac{S_1}{S_2} cosh\, b_1X\right) e^{-iaX} + (\frac{b_1}{b_2}\frac{2ia}{b_2} sin\, b_2X - \frac{S_1}{S_2} cos\, b_2X)e^{iaX}\right) \quad (12)$$

Assume:

- $S_3 = (\frac{S_1}{S_2}\frac{b_2}{ia} - \frac{b_1}{b_2})$
- At X=L

$$0= ((S_4 \sinh b_1\mathrm{L} + S_5 \cosh b_1\mathrm{L})\, e^{-ia\mathrm{L}} + (S_6 \sin b_2 l + S_7 \cos b_2 l)e^{ia\mathrm{L}}) \quad (13)$$

- $S_1 = (e^{-iaL}\, sinh\, b_1L - \frac{b_1}{b_2} e^{iaL}\, sin\, b_2L)$
- $S_2 = (e^{-iaL}\, cosh\, b_1L - e^{iaL}\, cos\, b_2L + \frac{b_2}{ia} e^{iaL}\, sin\, b_2L)$
- $S_3 = \left(\frac{S_1}{S_2}\frac{b_2}{ia} - \frac{b_1}{b_2}\right)$
- $S_4 = b_1^2 - a^2 - 2iab_1\frac{S_1}{S_2}$
- $S_5 = \frac{S_1}{S_2} b_1^2 - a^2\frac{S_1}{S_2} - 2iab_1$
- $S_6 = 2\frac{S_1}{S_2} b_2 ia - S_3 b_2^2 - a^2 S_3$
- $S_7 = 2iaS_3b_2 + \frac{S_1}{S_2} b_2^2 + a^2\frac{S_1}{S_2}$
- $\dot{W(X)} = A((\left(\frac{S_1}{S_2} b_1 - ia\right) sinh\, b_1\, X + \left(b_1 - ia\frac{S_1}{S_2}\right) cosh\, b_1X)\, e^{-iaX} + \left(\left(\frac{S_1}{S_2} b_2 + iaS_3\right) sin\, b_2X + (S_3b_2 - ia\frac{S_1}{S_2}\right) cos\, b_2X)e^{iaX}))$
- $\ddot{W(X)} = A((S_4\, sinh\, b_1X + S_5\, cosh\, b_1X)\, e^{-iaX} + (S_6\, sin\, b_2X + S_7\, cos\, b_2X)e^{iaX})$

2.5 Fluid Discharge Velocity

For a simply supported pipe, the natural frequency and corresponding fluid flow rate can be expressed as follows [26]:

$$\omega = \frac{\pi^2}{L^2}\sqrt{\frac{IE}{M_t}} \quad (14)$$

The mass per unit length of the composite pipe and the conveyed fluid is expressed as follows:

$$M_t = \rho_f \frac{\pi}{4} D_i^2 + \rho\frac{\pi}{4}\,(D_o^2 - D_i^2) \quad (15)$$

$$V = \frac{\pi}{L}\sqrt{\frac{IE}{\rho_f A}} \quad (16)$$

Equation (16), E represents the Young's modulus of the pipe material, I denote the moment of inertia, L is the length of the nanocomposite pipe, ρf corresponds to the density of the flowing fluid, and A indicates the cross-sectional area of the nanocomposite pipe.

2.6 Solve Pipe Axial tensile stress

The axial stress (σa) in a pipe can be derived from fundamental principles of mechanics. Consider a pipe with outer radius ro , inner radius ri , length L, and an applied axial force P. The derivation proceeds step by step as follows:

$$\boldsymbol{\sigma}_{axial} = \frac{Axial\ Force}{Cross\ sectional\ Area, A} \tag{17}$$

Where; $A = \pi(r_0^2 - r_i^2)$

This equation indicates that the axial stress in a pipe subjected to an axial force is directly proportional to the applied force and inversely proportional to the annular cross-sectional area.

$$\boldsymbol{\sigma}_{axial} = \frac{P}{\pi(r_0^2 - r_i^2)} \tag{18}$$

2.7 Solve The Ultimate Tensile Strain of Pipe

The ultimate tensile strain corresponds to the material's ultimate tensile strength (UTS) prior to failure. Strain is defined as the rate of elongation relative to the original length, and the axial strain (ε) is expressed as follows:

$$\varepsilon = \frac{\Delta L}{L} \tag{19}$$

where: ε = axial strain, L = original length of the pipe.

$$\boldsymbol{\sigma}_u = \frac{P_u}{\pi(r_0^2 - r_i^2)} \tag{20}$$

At ultimate tensile strength, the axial stress reaches its maximum value. Here, P_u represents the ultimate tensile load. Within the elastic region, stress and strain are related according to Hooke's law:

$$\sigma = E_\varepsilon \tag{21}$$

where: E = Young's modulus (modulus of elasticity). At the point of ultimate tensile stress: $\sigma_u = E_{\varepsilon_u}$. Thus, substituting: $\varepsilon_u = \frac{\sigma_u}{E}$ $\sigma_u = \frac{P_u}{\pi(r_0^2 - r_i^2)}$

$$\varepsilon_u = \frac{P_u}{E\pi(r_0^2 - r_i^2)} \tag{22}$$

Table 1. Nomenclatures

Symbol	Meaning	Units
A	Pipe cross-section area	cm^2
b_1, b_2	General solution parameters	-
K	General solution parameter	-
L_c	Crack length	cm
Do	Pipe outer diameter	cm
Di	Pipe inner diameter	cm
h	Thickness of pipe	cm
Dc	The depth of the Crack	mm
E	Elastic modulus	N/m^2
$\boldsymbol{F_o}$	External force	N/m
I	The second moment of the area	m^4
L	Pipe length	cm
M	Bending moment	N.m
mp	Mass of pipe per unit length	Kg/m
mf	Fluid mass per unit length	Kg/m
M_t	Mass per unit length of the pipe and fluid	Kg/m
p	Internal pressure	N/m^2
V_P	Shear forces	N/m^2

$\boldsymbol{M_P}$	Prescribed moment	N.m
A,B,C,D	Constants	
$\boldsymbol{S_i}$	Roots of equations	
V	Velocity of fluid	m/sec
x	The position along the pipe.	m
x_c	The crack position.	m
X	Dimensionless coordinate	-
y	Lateral coordinate	-
Y	Dimensionless coordinate	-
W	Amplitude of response	mm
Re	Reynold Number	-

Table 2. The Greek symbols

Symbol	Meaning	Units
α	Parameter	-
ω	fundamental natural frequency	Rad/sec
Ω	Dimensionless fundamental natural frequency	-
ρ	Density of pipe	kg/m^3
ρf	Fluid density	kg/m^3
$\lambda_{1,2}$	Roots of a polynomial equation	-

2.8 Numerical Solution

The numerical study comprises two main investigations. The first aims to evaluate the effect of fluid flow velocity on the vibration characteristics and natural frequency of the pipe. The second investigates the influence of axial tensile stress and ultimate tensile strain on pipe behavior. Fluid mechanics principles were applied under varying flow conditions to analyze the relationship between natural frequencies and system response, considering flow velocities of 1 m/s (Re = 13,500) and 2 m/s (Re = 27,000). The analysis was conducted for a pipe composed of a PVC/CF/Gr blend, as illustrated in Figure 2.

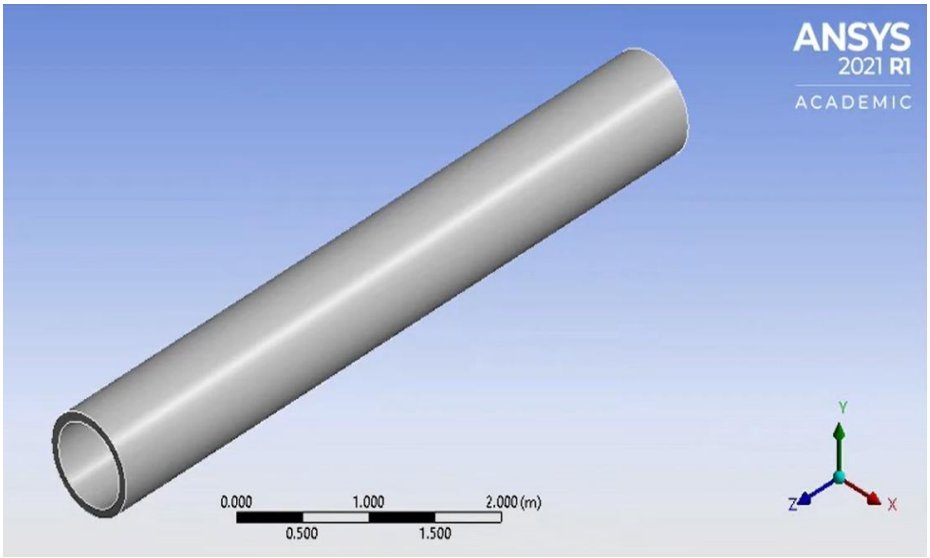

Fig. 2. Model of the composite pipe

In this study, the computational domain consists of a 100 cm-long pipe with inner and outer diameters of 4 cm and 6 cm, respectively. The materials used for pipe fabrication are summarized in Table 3. Numerical analysis was conducted using a finite element model (FEM) with a hexagonal mesh, implemented in ANSYS Workbench 21.0. The pipe was automatically meshed with a size of

0.9 mm, resulting in 26,588 elements and 215,629 nodes, as shown in Figure 3. Table **3**. Dimensions and properties of the pipe material.

Mechanical	Test value
Pipe material density	polyvinyl chloride/carbon fiber/graphene
Pipe density	----
Ultimate strength	251- 670 (MPa)
Ultimate elongation	(0.8 - 1.2) %
Pipe modulus of elasticity	(PVC/CF/Gr)
Pipe length (cm)	100 (cm)
Outer and inner diameters (cm)	6 (cm) and 4 (cm)
Fluid flow	Gas oil
Fluid density	0.822 (g/cm^3)

The numerical simulations included the calculation of the natural frequency of the composite pipe as well as the effects of fluid flow. Flow velocities of 1, 2, and 3 m/s were considered to investigate their influence on the dynamic behavior of the pipe. The numerical approach allows for a detailed assessment of the pipe's vibrational characteristics and the effects of fluid flow parameters and structural deformations [27].

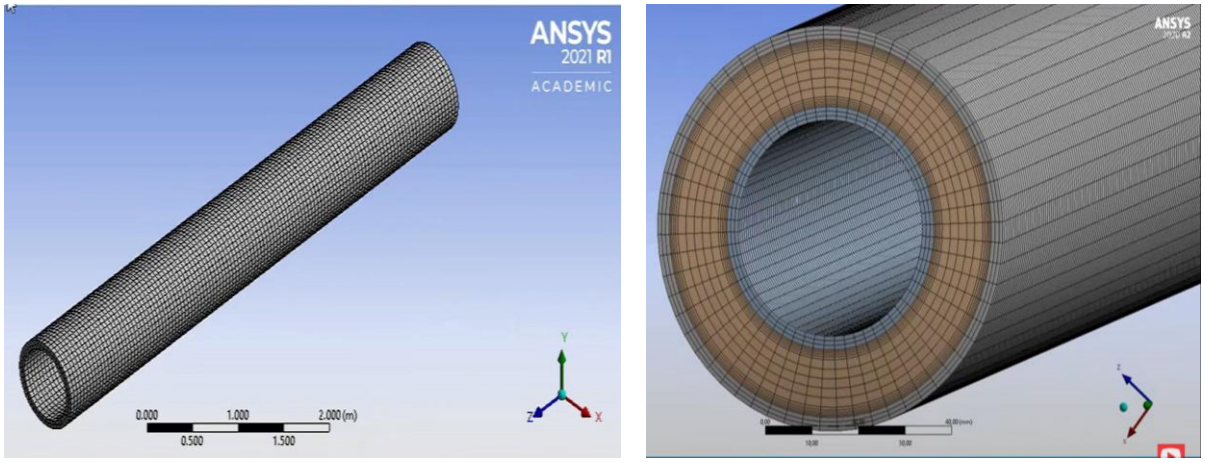

Fig. 3. The meshing of composite pipe installation

3. Results and Discussion

Table 4 presents the effect of fluid flow velocity on the natural frequency of a simply supported pipe at velocities of 1, 2, and 3 m/s. In addition to considering the material properties of the pipe and characteristics of the fluid flow, these effects were evaluated using both numerical and theoretical approaches and the results were systematically compared.

Table **4**. PVC/CF/Gr pipe natural frequency.

Fluid Velocity (m/s)	Analytical (Hz)	Numerical (Hz)	Discrepancy (%)
1	1287.4	1191.5	7.44
2	1173.3	1077.3	8.18
3	1058.5	980.5	7.36

Non-uniform flow distribution within the pipe induces internal pressure fluctuations, which in turn increase the pipe's vibrational response. Consequently, the natural frequencies of the pipe decrease as the fluid flow velocity varies. For instance, the fundamental frequency of a composite pipe is approximately 1287.4 Hz at a flow velocity of 1 m/s. When the velocity increases to 2 m/s, the frequency decreases by about 15%, reaching approximately 1173.3 Hz. These results demonstrate that higher flow velocities reduce the effective stiffness of the pipe structure. Figures 4, 5, and 6

illustrate the corresponding decrease in the fundamental natural frequency, as observed in both numerical and theoretical analyses.

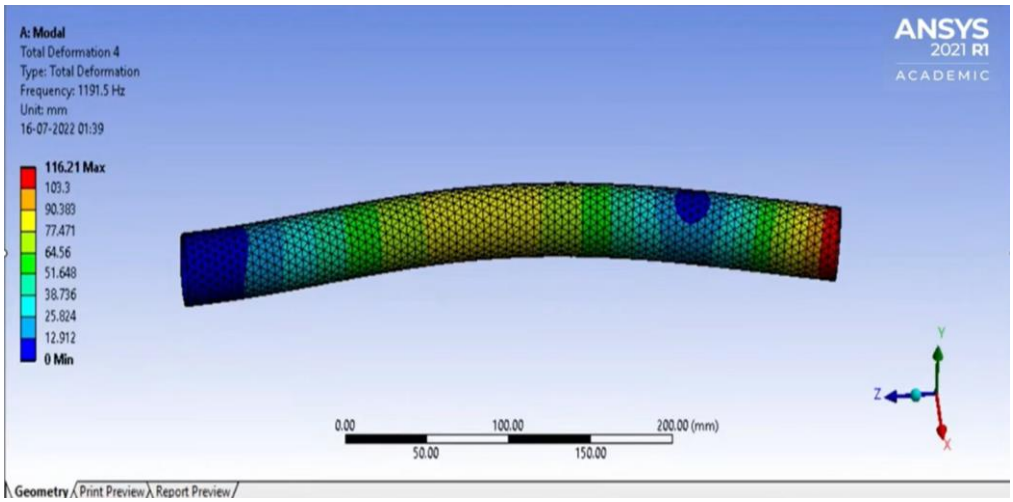

Fig. 4. PVC/CF/Gr pipe natural frequency and deflection

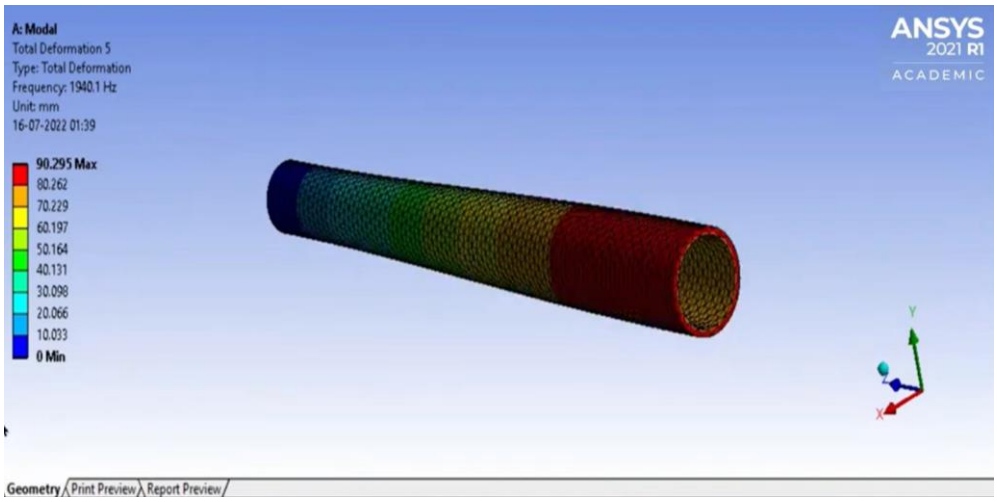

Fig. 5. PVC/CF/Gr pipe second mode shape (mm)

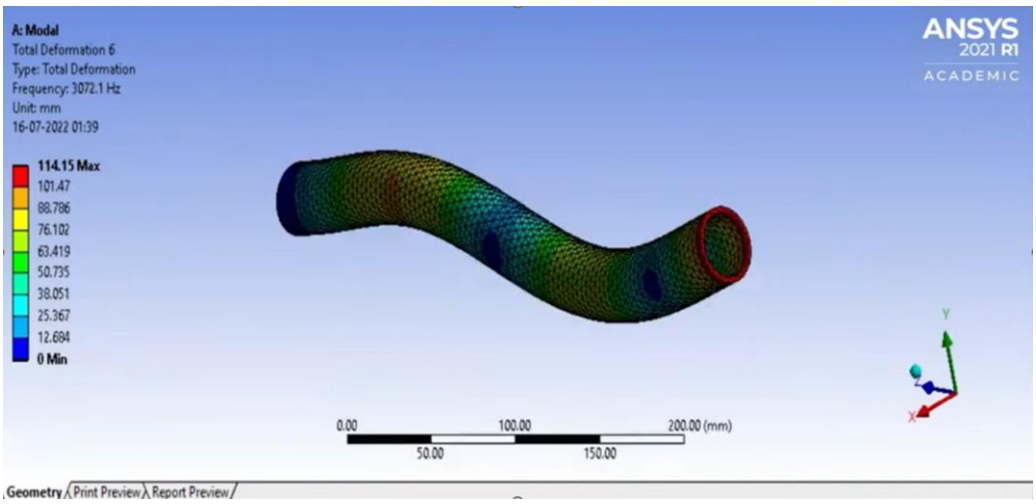

Fig. 6. PVC/CF/Gr pipe third mode shape (mm)

The results presented in Figures 7, 8, and 9 indicate that both Young's modulus and the ultimate tensile strength (UTS) of the pipe vary with the weight fraction of graphene (Gr). However, after two processing cycles, these improvements plateaued and remained relatively stable. The increase

in Young's modulus and ultimate tensile strength for the PVC/CF/Gr nanocomposite ranged from 7.7% to 19.5%. The maximum tensile strength achieved was 670.3 MPa for PVC/CF pipes containing 2 wt% graphene, demonstrating that increasing the graphene content enhances the mechanical properties. For comparison, an API version a pipe exhibited UTS of 330 MPa, while the PVC/CF composite without graphene showed a tensile strength of 251.9 MPa (Table 5), representing a significant improvement over high-grade API steel pipes and demonstrating their potential for pipeline applications in the oil and gas industry.

Tables 6and 7 further show that incorporating 2 wt% graphene significantly increased the stiffness of the pipe. The maximum allowable compressive strength of the pipes for various applications was also evaluated, with results indicating a peak at 2 wt. % graphene. These findings confirm that an optimal graphene content of 2% by weight provides the best enhancement in both tensile and compressive mechanical properties for the PVC/CF/Gr composite pipes.

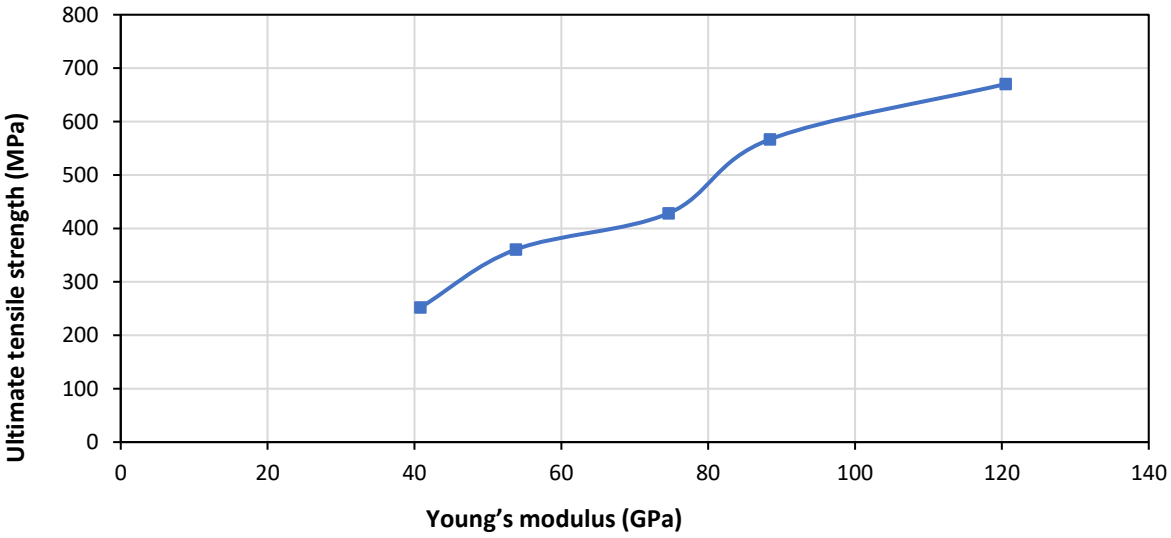

Fig. 7. The relationship between Young's modulus and Ultimate tensile strength for a composite pipe, PVC/CF/Gr

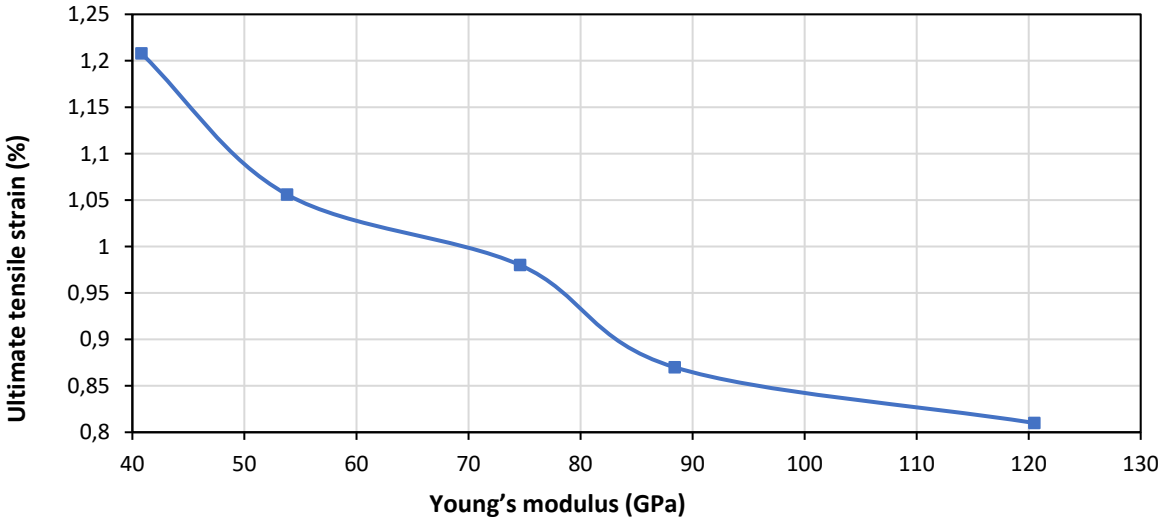

Fig. 8. The correlation between Young's modulus and the Ultimate tensile strain of the PVC/F/Gr composite pipe

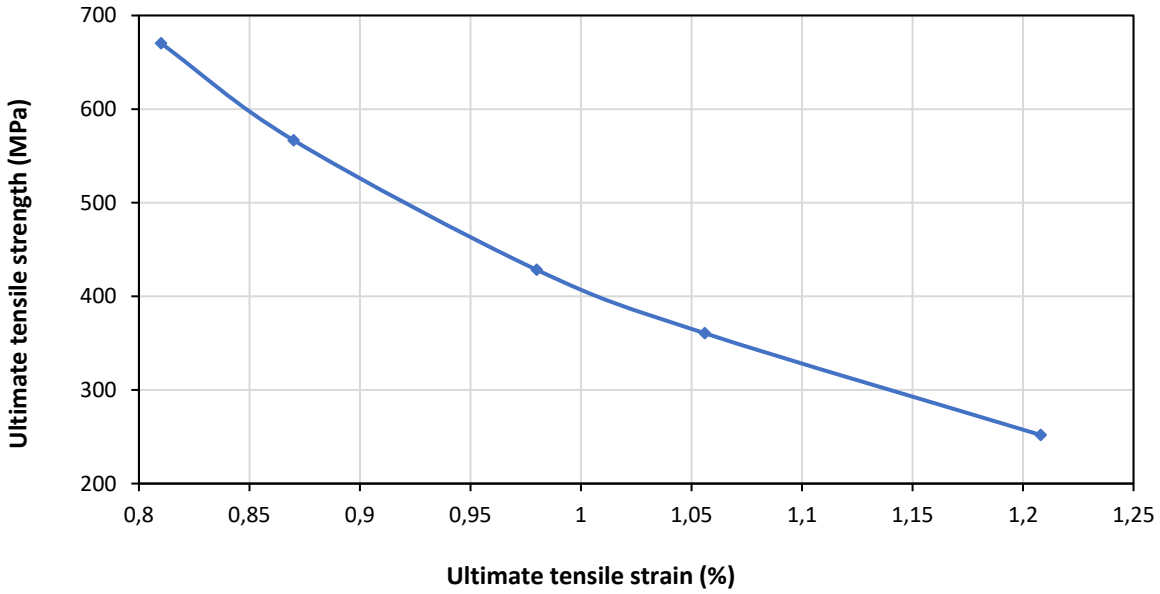

Fig. 9. The relationship between Ultimate tensile strength and the Ultimate tensile strain of the PVC/CF/Gr composite pipe

Table 5. PVC/CF/Gr pipe tensile strength and Young's modulus

Specimen	Young's modulus (GPa)	Ultimate tensile strength (MPa)	Ultimate tensile strain (%)
PVC-CF	40.8	251.9	1.208
0.5% Gr	53.8	360.6	1.056
1% Gr	74.6	428.3	0.98
1.5% Gr	88.4	566.7	0.87
2% Gr	120.5	670.3	0.81

Table 6. PVC/CF/Gr pipes' compressive strength for different weights of graphene

Specimen	Compressive strength (MPa)
PVC-CF	230.2
0.5% Gr	312.8
1% Gr	391.5
1.5% Gr	520.3
2% Gr	479.4

Table 7. PVC/CF/Gr pipe loading test for different weights of graphene

Specimen	Ultimate compressive load (N)	Stiffness (kPa)
PVC-CF	4270	190.7
0.5%Gr	5664	267.9
1% Gr	6848	338.8
1.5% Gr	7547	385.3
2% Gr	8115	412.7

4. Conclusion

This study investigated the mechanical and dynamic properties of pipes composed of polyvinyl chloride (PVC), carbon fiber (CF), and graphene (Gr) to assess their suitability for use in oil and gas pipelines. The key findings are as follows:

- In this study, the general solution of the vibration equation for conservative fluid-conveying pipes is derived. Based on this solution, the frequency equations of boundary conditions for a simply supported pipe transporting fluid are analytically obtained in terms of the pipe's governing parameters.
- Optimal enhancement in ultimate tensile strength was achieved with 2 wt% graphene, resulting in a 31% increase.
- The tensile strength of the composite pipes reached 670 MPa, representing a substantial improvement over high-quality API steel pipes, demonstrating their feasibility for oil and gas pipeline applications.
- The presence of a crack disrupts the flow distribution within the pipe. While the flow through an uncracked pipe remains continuous, the introduction of a crack leads to disturbances in the flow pattern. As the crack length and orientation vary, the flow distribution progressively transitions from a continuous to a discontinuous state. An increase in fluid flow velocity led to a decrease in the natural frequencies of the pipe.
- A comparison between theoretical analysis and numerical simulations for estimating pipe frequency under flow-induced vibration showed strong agreement, with a maximum deviation of approximately 8.18% across different flow velocities.
- Further investigations revealed notable improvements in the axial mechanical behavior of the composite pipes.
- The incorporation of graphene into the PVC/CF composite not only strengthened the matrix phase but also significantly improved the interfacial adhesion between the polymer matrix and the reinforcing fibers.

These results confirm that PVC/CF/Gr composite nano pipes exhibit superior mechanical performance, enhanced dynamic stability, and excellent engineering properties, making them highly suitable for next-generation pipeline systems intended for oil and gas transportation.

4.1 Future Work and Recommendations

Building upon the findings of this study, several directions for future research are recommended to further advance the understanding and application of PVC–Carbon Fiber–Graphene nanocomposite pipes in oil and gas systems:

- Experimental Validation: Conduct practical mechanical testing, including tensile, compressive, fatigue, and impact assessments, to validate the numerical and analytical results obtained in this study.
- Thermal and Environmental Effects: Investigate the influence of elevated temperatures, UV exposure, chemical interactions, and thermal cycling on the mechanical and vibration performance of the nanocomposite pipes.
- Fluid–Structure Interaction: Examine the interaction between transported fluids and the pipe walls, considering internal pressure fluctuations, turbulent flow, and multiphase transport, to assess their impact on stress distribution and vibration behavior.
- Nanofiller Optimization: Explore a broader range of graphene and carbon fiber concentrations, as well as hybrid or functionalized nanofillers, to optimize mechanical performance, stiffness, and cost-efficiency.
- Corrosion and Wear Resistance: Evaluate long-term durability, erosion, and chemical resistance of the nanocomposite pipes, including the potential benefits of surface treatments or protective coatings.
- Manufacturing Scale-Up: Assess the effects of industrial-scale fabrication methods, such as injection molding, extrusion, or filament winding, on mechanical properties, material uniformity, and structural integrity.

Acknowledgement

The authors express their sincere gratitude to all the professors who supervised and supported the organization of this distinguished scientific conference. Special thanks are extended to the Ministry of Higher Education and Scientific Research, the Iraqi Geotechnical Society, Komar University of Science and Technology, the publishing journal, and all other scientific institutions involved in facilitating the publication of this paper.

References

[1] Nawaz M, Yusuf N, Habib S, Shakoor R, Ubaid F. Development and properties of polymeric nanocomposite coatings. Polymers. 2019;11(5):852. https://doi.org/10.3390/polym11050852

[2] Radhamani AV, Chung HC, Ramakrishna S. Nanocomposite coatings on steel for enhancing the corrosion resistance: a review. J Compos Mater. 2019;54(5):681-701. https://doi.org/10.1177/0021998319857807

[3] Pourhashem S, Vaezi MR, Rashidi A, Bagherzadeh MR. Exploring corrosion protection properties of solvent-based epoxy-graphene oxide nanocomposite coatings on mild steel. Corros Sci. 2017;115:78-92. https://doi.org/10.1016/j.corsci.2016.11.008

[4] Shankarachar SM, Radhakrishina M, Babu PR. An experimental study of flow induce vibration of elastically restrained pipe conveying fluid. In: Proceedings of the 15th International Mechanical Engineering Congress and Exposition (IMECE15); 2015 Nov 13-19; Houston, TX, USA.

[5] Jweeg MJ, Mohammad SK, Alnomani SN. Dynamic analysis of a rotating stepped shaft with and without defects. In: 3rd International Conference on Engineering Sciences. IOP Conf Ser: Mater Sci Eng. 2020;671:012004. https://doi.org/10.1088/1757-899X/671/1/012004

[6] TabkhPaz M, Park DY, Lee PC, Hugo R, Park SS. Development of nanocomposite coatings with improved mechanical, thermal, and corrosion protection properties. J Compos Mater. 2018;52(8):1045-1060. https://doi.org/10.1177/0021998317720001

[7] Yu YH, Lin YY, Lin CH, Chan CC, Huang YC. High-performance polystyrene/graphene-based nanocomposites with excellent anti-corrosion properties. Polym Chem. 2014;5:535-550. https://doi.org/10.1039/C3PY00825H

[8] Liu J, Liu T, Guo Z, Guo N, Lei Y, Chang X, et al. Promoting barrier performance and cathodic protection of zinc-rich epoxy primer via single-layer graphene. Polymers. 2018;10(6):591. https://doi.org/10.3390/polym10060591

[9] Pathak AK, Garg H, Singh M, Yokozeki T, Dhakate SR. Enhanced interfacial properties of graphene oxide incorporated carbon fiber reinforced epoxy nanocomposite: a systematic thermal properties investigation. J Polym Res. 2019;26:1-13. https://doi.org/10.1007/s10965-018-1668-2

[10] Samsudin MS, Mahtar MA, Leong KH. Barrier and thermal performance of graphene-HDPE nanocomposites for pipeline liner application. In: SPE Middle East Oil and Gas Show and Conference; 2019 Mar; Manama, Bahrain. Paper No: SPE-195069-MS. p. 18-21. https://doi.org/10.2118/195069-MS

[11] Pourhashem S, Rashidi A, Vaezi MR. Excellent corrosion protection performance of epoxy composite coatings filled with amino-silane functionalized graphene oxide. Surf Coat Technol. 2017;317:1-9. https://doi.org/10.1016/j.surfcoat.2017.03.050

[12] Karsli NG, Yesil S, Aytac A. Effect of hybrid carbon nanotube/short glass fiber reinforcement on the properties of polypropylene composites. Compos Part B Eng. 2014;63:154-160. https://doi.org/10.1016/j.compositesb.2014.04.006

[13] Yip MC, Lin YC, Wu CL. Effect of multi-walled carbon nanotubes addition on mechanical properties of polymer composites laminate. Polym Polym Compos. 2011;19:131-140. https://doi.org/10.1177/0967391111019002-313

[14] Prusty RK, Ghosh SK, Rathore DK, Ray BC. Reinforcement effect of graphene oxide in glass fiber/epoxy composites at in-situ elevated temperature environments: emphasis on graphene oxide content. Compos Part A Appl Sci Manuf. 2017;95:40-53. https://doi.org/10.1016/j.compositesa.2017.01.001

[15] Patil A, Patel A, Sharma PK. Effect of carbon nanotube on mechanical properties of hybrid polymer matrix nanocomposites at different weight percentages. Mater Today Proc. 2018;5(2):6401-6405. https://doi.org/10.1016/j.matpr.2017.12.251

[16] Rajabi M, Rashed GR, Zaarei D. Assessment of graphene oxide/epoxy nanocomposite as corrosion resistance coating on carbon steel. Corros Eng Sci Technol. 2015;50:509-516. https://doi.org/10.1179/1743278214Y.0000000232

[17] Brandenburg RF, Lepienski CM, Becker D, Coelho LAF. Influence of mixing methods on the properties of high-density polyethylene nanocomposites with different carbon nanoparticles. Matéria (Rio J). 2017;22:e11888. https://doi.org/10.1590/s1517-707620170004.0222

[18] Aldajah S, Haik Y. Transverse strength enhancement of carbon fiber reinforced polymer composites by means of magnetically aligned carbon nanotubes. Mater Des. 2012;34:379-383. https://doi.org/10.1016/j.matdes.2011.07.013
[19] Saad ALG, Sayed WM, Ahmed MGM, Hassan AM. Preparation and properties of some filled poly(vinyl chloride) compositions. J Appl Polym Sci. 1999;73:2657-2670. https://doi.org/10.1002/(SICI)1097-4628(19990923)73:13<2657::AID-APP14>3.0.CO;2-7
[20] Nawaz K, Ayub M, Ul-Haq N, Khan MB, Khan Niazi MB. The effect of graphene nanosheets on the mechanical properties of polyvinylchloride. Polym Compos. 2016;37:1572-1576. https://doi.org/10.1002/pc.23328
[21] Aljaafari A, Abu-Abdeen M, Aljaafari M. Mechanical and electrical properties of poly(vinyl chloride) loaded with carbon nanotubes and carbon nanopowder. J Thermoplast Compos Mater. 2011;25:679-699. https://doi.org/10.1177/0892705711412650
[22] Xiao Y, Chen Z, Xin B, Li L. Preparation and characterization of graphene enriched poly(vinyl chloride) composites and fibers. J Text Inst. 2017;109:1-8. https://doi.org/10.1080/00405000.2017.1398059
[23] Kuram E, Ozcelik B, Yilmaz F. The influence of recycling number on the mechanical, chemical, thermal and rheological properties of poly(butylene terephthalate)/polycarbonate binary blend and glass-fiber reinforced composite. J Thermoplast Compos Mater. 2016;29:1443-1457. https://doi.org/10.1177/0892705715569823
[24] Kadam PG, Mhaske ST. Effect of extrusion reprocessing on the mechanical, thermal, rheological and morphological properties of nylon 6/talc nanocomposites. J Thermoplast Compos Mater. 2016;29:960-978. https://doi.org/10.1177/0892705714551591
[25] Liu JB, Yue QB, Dong RZ, Zhang Q. The analysis of vortex-induced vibration of the flexible pipe in a cylindrical fluid field with cross flow. J Vibroengineering. 2016;18. https://doi.org/10.21595/jve.2016.16547
[26] Ismail MR. Evaluating the dynamical behavior and stability of pipes conveying fluid [PhD thesis]. Baghdad: Al-Nahrain University, Mechanical Engineering; 2011.
[27] Hunain MB. The fundamental natural frequency and critical flow velocity evaluation of a simply supported stepped pipe conveying fluid. J Babylon Univ Eng Sci. 2017;25(5).